Communication: Identification of the molecule–metal bonding geometries of molecular nanowires

Firuz Demir[a] and George Kirczenow[b]
Department of Physics, Simon Fraser University, Burnaby, British Columbia V5A 1S6, Canada

(Received 26 January 2011; accepted 8 March 2011; published online 23 March 2011)

Molecular nanowires in which a single molecule bonds chemically to two metal electrodes and forms a stable electrically conducting bridge between them have been studied intensively for more than a decade. However, the experimental determination of the bonding geometry between the molecule and electrodes has remained elusive. Here we demonstrate by means of *ab initio* calculations that inelastic tunneling spectroscopy (IETS) can determine these geometries. We identify the bonding geometries at the gold–sulfur interfaces of propanedithiolate molecules bridging gold electrodes that give rise to the specific IETS signatures that were observed in recent experiments. © *2011 American Institute of Physics*. [doi:10.1063/1.3571473]

Molecular nanowires in which a single organic molecule bonds chemically to two metal electrodes and forms a stable electrically conducting bridge between them have attracted a great deal of attention[1] because of their fundamental interest and potential applications as single-molecule nanoelectronic devices. However, a single molecule located between two electrodes is not accessible to scanning microprobes that can measure atomic scale structure. Thus, definitive determination of the bonding geometries at the molecule–electrode interfaces of single-molecule nanowires continues to be elusive despite being critically important for understanding electrical conduction through molecular wires quantitatively and for gaining control over their structures for device applications.

In the case of single-molecule nanowires bridging gold electrodes and thiol bonded to them, possible bonding geometries include those in which a sulfur atom of the molecule is located at a *top* site over a particular gold surface atom or over a *bridge* site between two gold atoms or over a *hollow* site between three gold atoms.[1] However, there have been no direct experiments determining which (if any) of these possibilities are actually realized. For molecules amine linked to gold electrodes it has been argued that top site bonding is the most probable,[2] but *direct* experimental evidence of this has also been lacking.

The excitation of molecular vibrations (phonons) by electrons passing through single-molecule nanowires gives rise to conductance steps in the low temperature current–voltage characteristics of the nanowires. Inelastic tunneling spectroscopy (IETS) experiments have detected these steps and measured the energies of the emitted phonons.[1] These experiments proved that particular molecular species are involved in electrical conduction through metal–molecule–metal junctions.[3] Density functional theory (DFT) based simulations[4–6] have accounted for many features of the IETS data. However, the possibility that IETS might identify the *bonding geometries* at the molecule–metal *interfaces* and thus resolve the long standing problem of the molecule–electrode structure has not been investigated in the literature. We explore it in this paper and identify for the first time the molecule-contact bonding geometries that were realized in experiments on an organic molecule bridging metal contacts. We consider one of the simplest organic molecules, 1,3-propanedithiolate (PDT), bridging gold electrodes for which detailed experimental IETS data are available.[7]

We focus on inelastic tunneling processes that are sensitive to the structure of the gold–sulfur interfaces, i.e., those that involve excitation of vibrational modes with strong amplitudes on the sulfur atoms. Therefore, it is necessary to calculate accurate equilibrium geometries and also the frequencies and atomic displacements from equilibrium for the vibrational modes of the *whole* system, including both the molecule and the gold electrodes. We do this by performing *ab initio* DFT calculations[8] for *extended* molecules consisting of the PDT molecule and two finite clusters of gold atoms that the molecule connects, relaxing this entire structure. By carrying out systematic DFT studies of extended molecules with gold clusters of different sizes (up to 13 gold atoms per cluster) we establish that our conclusions are independent of the cluster size for the larger clusters that we study and, thus, are applicable to molecules bridging the nanoscale tips of experimentally realized macroscopic gold electrodes.

We found extended molecules whose sulfur atoms bond to the gold clusters over bridge sites to have lower energies than those with top site bonding by at least 0.76 eV. Extended molecules for which DFT geometry relaxations were started with the sulfur atoms over hollow sites on the surfaces of close packed gold clusters invariably relaxed to bridge bonding site geometries. While we found it possible to generate examples of relaxed extended molecules with each sulfur atom bonding to three gold atoms (i.e., hollow site bonding) the structures of the gold clusters near these bonding sites were much more open than that of a fcc gold crystal. The energies of these structures were also higher than those of either bridge or top site bonded extended molecules. Because of the much greater

[a]Electronic mail: fda3@sfu.ca.
[b]Electronic mail: kirczeno@sfu.ca.

fragility and higher energies of hollow site bonded structures relative to bridge and top site bonding we will focus primarily on bridge and top site bonding but will revisit hollow site bonding near the end of this paper.

After identifying the normal modes of the extended molecule that have the largest vibrational amplitudes on the sulfur atoms and calculating the frequencies of those modes as is outlined above, we determine which of these modes has the strongest IETS intensity, i.e., it gives rise to the largest conductance step height as the bias voltage applied across the extended molecule is varied.

We calculate the IETS intensities perturbatively in the spirit of an approach proposed by Troisi *et al.*[9] who transformed the problem of calculating IETS intensities into an *elastic* scattering problem. However, we formulate our IETS intensities explicitly in terms of elastic electron transmission amplitudes t_{ji}^{el} through the molecular wire. We find the height δg_α of the conductance step due to the emission of phonons of vibrational mode α to be

$$\delta g_\alpha = \frac{e^2}{2\pi\omega_\alpha} \lim_{A\to 0} \sum_{ij} \frac{v_j}{v_i} \left| \frac{t_{ji}^{el}(\{A\mathbf{d}_{n\alpha}\}) - t_{ji}^{el}(\{\mathbf{0}\})}{A} \right|^2, \qquad (1)$$

at low temperatures. Here $t_{ji}^{el}(\{\mathbf{0}\})$ is the elastic electron transmission amplitude through the molecular wire in its equilibrium geometry from state i with velocity v_i in the electron source to state j with velocity v_j in the electron drain. $\mathbf{d}_{n\alpha}$ represents the displacements from their equilibrium positions of the atoms n of the extended molecule in normal mode α normalized so that $\sum_n m_n \mathbf{d}_{n\alpha'}^* \cdot \mathbf{d}_{n\alpha} = \delta_{\alpha',\alpha}$ where m_n is the mass of atom n. ω_α is the frequency of mode α. $t_{ji}^{el}(\{A\mathbf{d}_{n\alpha}\})$ is the elastic electron transmission amplitude through the molecular wire with each atom n displaced from its equilibrium position by $A\mathbf{d}_{n\alpha}$ where A is a small parameter. Our formal derivation of Eq. (1) will be presented elsewhere; here we point out that Eq. (1) is plausible intuitively in a similar way to the result of Troisi *et al.*:[9] Eq. (1) states that in the leading order of perturbation theory the scattering amplitude for *inelastic* transmission of an electron through the molecular wire is proportional to the change in the *elastic* amplitude for transmission through the wire if its atoms are displaced from their equilibrium positions as they are when vibrational mode α is excited.

In our evaluation of t_{ji}^{el} in Eq. (1) the coupling of the extended molecule to the macroscopic electron reservoirs was treated as in previous work[10–12] by attaching a large number of semi-infinite quasi-one-dimensional ideal leads to the valence orbitals of the outer gold atoms of the extended molecule. The transmission amplitudes t_{ji}^{el} were then found by solving the Lippmann–Schwinger equation:

$$|\Psi\rangle = |\Phi_0\rangle + G_0(E)W|\Psi\rangle, \qquad (2)$$

where $|\Phi_0\rangle$ is an electron eigenstate of an ideal left lead that is decoupled from the extended molecule, $G_0(E)$ is the Green's function for the decoupled system of the ideal leads and the extended molecule, W is the coupling between the extended molecule and leads, and $|\Psi\rangle$ is the scattering eigenstate of the complete coupled system. In evaluating $G_0(E)$ semiempirical extended Hückel theory[13,14] was used to model the electronic structure of the extended molecule. Previous calculations based on extended Hückel theory have yielded elastic tunneling conductances in agreement with experiment for molecules thiol bonded to gold electrodes[12,15,16] and have accounted for transport phenomena observed in molecular arrays on silicon[10] as well as electroluminescence data,[17] current–voltage characteristics[17] and STM images[18] of molecules on complex substrates.

We calculated the zero bias tunneling conductances for gold-PDT-gold molecular wires from the Landauer formula $g = g_0 \sum_{ij} |t_{ji}^{el}(\{\mathbf{0}\})|^2 v_j/v_i$ with $g_0 = 2e^2/h$, evaluating the elastic transmission amplitudes $t_{ji}^{el}(\{\mathbf{0}\})$ as described above and found values in the range $g = 0.0012$–$0.0014 g_0$ and 0.0012-$0.0020 g_0$ for top site and bridge site bonded molecules, respectively. The degree of agreement between these theoretical values and the experimental value[7] $0.006 \pm 0.002 g_0$ is typical of that in the literature[19] on molecules thiol bonded to gold electrodes; as in previous studies[19] comparing the elastic conductance calculations with experiment does not reveal which bonding geometry was realized experimentally.

We then calculated the vibrational modes, their frequencies, and IETS intensities as described above for many gold-PDT-gold extended molecules with various gold–sulfur bonding geometries and compared our results with the experimental data of Hihath *et al.*[7] Our calculations showed that the modes with strong amplitudes of vibration on the sulfur atoms that have the largest IETS intensities fall within the phonon energy range of a prominent feature of the experimental IETS phonon histogram[7] that extends from 39 to 52 meV.

We show the vibrational modes that we find in this energy range for representative top site and bridge site bonding geometries in Fig. 1. The calculated IETS spectra (phonon energies and IETS intensities) in the same energy range are shown in Fig. 2 for several extended molecules with gold clusters of various sizes together with the experimental IETS phonon mode histogram.[7]

The mode with the strongest calculated IETS intensities in Fig. 2 is mode I shown in the top row of Fig. 1. In this mode the sulfur atoms have the strongest vibrational amplitudes and move in antiphase, approximately along the axis of the molecule. The other mode in this energy range is mode II shown in the lower row of Fig. 1. It is similar to mode I except that the sulfur atoms move in phase with each other.

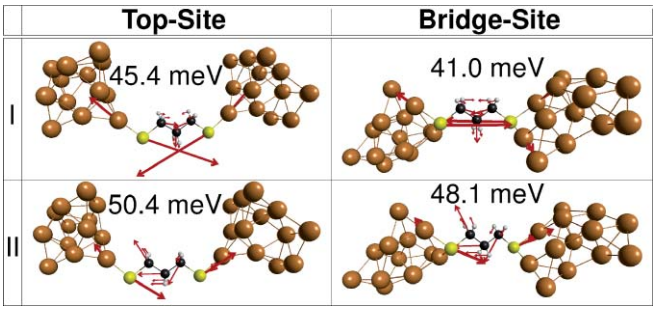

FIG. 1. Calculated vibrational modes in phonon energy range from 39 to 52 MeV for trans-PDT bridging gold nanoclusters with sulfur atoms bonded to gold in top-site and bridge-site geometries. Red arrows show un-normalized atomic displacements. Mode I has the stronger IETS intensity (Ref. 20).

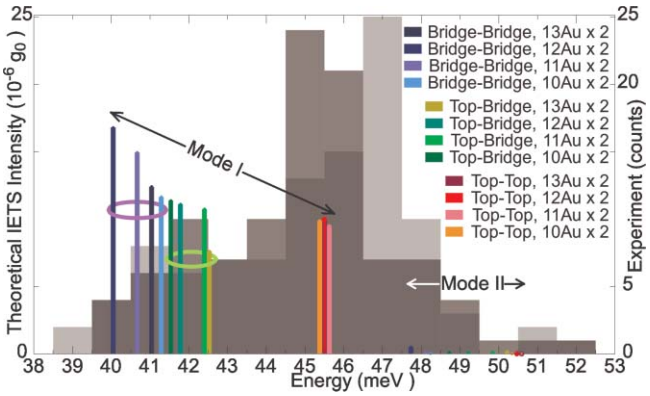

FIG. 2. Calculated phonon energies and IETS intensities for trans-PDT molecules linking pairs of gold clusters with between 10 and 13 Au atoms in each cluster. Results are shown for both sulfur atoms bonding to the gold in top-site and bridge-site geometries and for top site bonding to one gold cluster and bridge site bonding to the other. The two ellipses enclose the calculated type I mode IETS spectra for pure bridge and mixed top-bridge bonding geometries, respectively, for extended molecules with gold clusters containing various numbers of gold atoms. The experimental IETS phonon mode histogram of Hihath *et al.* (Ref. 7) is shown in (darker, lighter) grey for (positive, negative) bias voltages.

As is seen in Fig. 2 the calculated IETS intensities for mode II are much weaker than those for mode I for both top and bridge site bonding.

The reason for this difference between the IETS intensities of modes I and II can be understood intuitively by considering the nature of the motion in relation to Eq. (1): Since in mode I the two sulfur atoms move in antiphase the gold–sulfur distances for both sulfur atoms either increase or decrease *together* as the extended molecule vibrates. These distances can be regarded as the widths of tunnel barriers between the molecule and the two gold electrodes. Thus, the motions of the two sulfur atoms act *in concert* to widen or narrow *both* tunnel barriers together and, therefore, to weaken or strengthen the electron transmission amplitude through the molecular wire. Thus, the magnitude of the difference between the elastic electron transmission amplitudes through the molecular wire in its equilibrium and vibrating geometries $|t_{ji}^{el}(\{A\mathbf{d}_{n\alpha}\}) - t_{ji}^{el}(\{\mathbf{0}\})|$ in Eq. (1) is enhanced. By contrast in mode II when the gold–sulfur distance for one sulfur atom increases the gold–sulfur distance for the other sulfur atom decreases. Thus, the effects of the motions of the two sulfur atoms on the elastic transmission amplitude through the molecular wire tend to cancel. Thus $|t_{ji}^{el}(\{A\mathbf{d}_{n\alpha}\}) - t_{ji}^{el}(\{\mathbf{0}\})|$ in Eq. (1) is smaller for mode II than mode I and, therefore, the IETS intensity δg_α for mode II is *much* smaller as is seen in Fig. 2.

Comparison of the calculated IETS spectra in Fig. 2 with the experimental phonon mode histogram[7] indicates that vibrational mode I contributed most of the counts recorded in the histogram in the energy range shown. This is consistent with the fact that the calculated IETS intensities for mode I are much stronger than those for mode II and therefore mode I should be more readily detected in experimental IETS measurements.

The theoretical results for the dominant IETS mode I in Fig. 2 reveal that the prominent features of the histogram[7] can be explained as arising from PDT molecules that bond to the gold electrodes in *different* ways: The main peak in the experimental histogram[7] that is centered at ~46 meV matches our theoretical result for trans-PDT molecules that bond to both gold electrodes in the top site geometry. The weaker peak centered near 42 meV matches our predictions for molecules that bond to one gold electrode in the top site geometry and to the other electrode in the bridge site geometry. The shoulder of the experimental histogram[7] at lower phonon energies between 39.5 and 41.5 meV corresponds to our results for molecules bonding to both electrodes in the bridge site geometry.

Notice that our theoretical results for phonon mode I of PDT molecules bonded to both electrodes in the top site geometry (the feature near 45.5 meV in the theoretical spectra in Fig. 2) are very well converged with respect to increasing gold cluster size: Both the calculated phonon energies and the IETS intensities are almost independent of the gold cluster size in the size range shown (10–13 gold atoms per cluster). The calculated phonon energy of this dominant mode matches the phonon energy of the main peak of the experimental phonon mode histogram in Fig. 2 very well. It is also well separated from the calculated phonon energies of the dominant mode I for the pure bridge and mixed bridge–top site bonded geometries. As a check we calculated the vibrational mode energies and IETS intensities for a few examples of extended molecules using a different density functional[8] and found similar results. Thus, our results identify *unambiguously* those specific realizations of the molecular wire that gave rise to the counts within the main peak of the experimental histogram[7] reproduced in Fig. 2 as being those in which both sulfur atoms bonded to the gold electrodes in the top site geometry. The calculated mode I phonon energies in Fig. 2 for pure bridge site-bonded and mixed bridge-top site-bonded molecular wires show more variation with gold cluster size than do the calculated mode I phonon energies for molecules in the pure top site-bonded geometry. However, the ranges in which the calculated energies of the mode I phonons for pure bridge site-bonded and mixed bridge/top site-bonded molecular wires occur do not overlap. Also, the calculated phonon energies for these modes and bonding geometries do not show any systematic trend toward higher or lower values with increasing cluster size. Thus, it is plausible that the weaker peak centered near 42 meV in the experimental histogram is due to mixed bridge/top site-bonded molecular wires and the lower energy shoulder between 39.5 and 41.5 meV in the histogram is due to pure bridge site-bonded wires.

As the gold-PDT-gold junction was stretched in the experiment[7] the energy of the prominent phonon mode in the IETS spectrum was observed to switch from ~42 to ~46 meV. It was conjectured[7] that this switch may be due to a change in the contact configuration or between gauche and trans molecular geometries, but no evidence supporting either possibility was offered and the contact configurations involved were not identified.[7] Here we point out that trans-PDT molecules switching from the mixed top–bridge site bonding (calculated phonon energy ~42 meV) to the pure top site bonding geometry (calculated phonon energy ~45.5 meV)

accounts for this observed transition. Our calculated distance between the gold clusters of the extended molecule is larger for pure top site bonding than for mixed top–bridge bonding. This is consistent with the transition from mixed top–bridge to pure top site bonding occurring as the molecular junction is stretched. For longer chain alkanedithiolates, it has been conjectured[21] that switching from mixed hollow site–top site bonding to top site bonding at both gold electrodes may occur. This conjecture does not account for the observed switch from the ~42 meV mode to the ~46 meV mode in the gold-PDT-gold junctions: As noted above, we find hollow-site bonding to be much more fragile (and thus less likely to be realized) than bridge site bonding. We also find the energy of the mode of the mixed hollow-top structure with the strongest IETS intensity to match *neither* the ~42 meV nor the ~46 meV phonon mode. The theoretical results presented above are for trans-PDT molecules. We have also studied many gold-PDT-gold structures with molecular gauche defects and find that such structures also do not account for the observed[7] switching from the ~42 meV phonon mode to the ~46 meV phonon mode.

In conclusion: We have shown inelastic tunneling spectroscopy to be able to distinguish between different bonding geometries of the molecule and metal contacts in single-molecule molecular wires, an important and previously elusive goal in the field of single-molecule nanoelectronics. We have definitively identified particular realizations of gold-propanedithiolate-gold molecular wires in a recent experiment[7] in which the molecule bonded to a single gold atom of each electrode. The success of our approach rests on the fact that *ab initio* density functional theory calculations of vibrational modes and their frequencies are known to be accurate because in the Born–Oppenheimer approximation they are electronic *ground state total energy* calculations.[1,5] We rely on transport calculations only for the identification of the phonon mode in a particular frequency range that has the largest IETS intensity, and our identification of this mode is also supported by physical reasoning.

This research was supported by CIFAR, NSERC, and Westgrid. We thank J. Hihath, N. J. Tao, E. Emberly, N. R. Branda, V. E. Williams, and A. Saffarzadeh for helpful discussions and J. Hihath and N. J. Tao for providing to us their data from Ref. 7 in digital form.

[1] For a review see G. Kirczenow, *The Oxford Handbook of Nanoscience and Technology: Volume 1: Basic Aspects* (Oxford University Press, Oxford, UK, 2010), Chap. IV.
[2] M. S. Hybertsen, L. Venkataraman, J. E. Klare, A. C. Whalley, M. L. Steigerwald, and C. Nuckolls, J. Phys. Condens. Matter **20**, 374115 (2008).
[3] J. G. Kushmerick, J. Lazorcik, C. H. Patterson, R. Shashidhar, D. S. Seferos, and G. C. Bazan, Nano Lett. **4**, 639 (2004); W. Wang, T. Lee, I. Kretzschmar, and M. A. Reed, *ibid.* **4**, 643 (2004).
[4] A. Pecchia and A. Di Carlo, Nano Lett. **4**, 2109 (2004).
[5] A. Troisi and M. A. Ratner, Phys. Rev. B **72**, 033408 (2005); Phys. Chem. Chem. Phys. **9**, 2421 (2007).
[6] N. Sergueev, D. Roubtsov, and H. Guo, Phys. Rev. Lett. **95**, 146803 (2005); C. Benesch, M. Čížek, M. Thoss, and W. Domcke, Chem. Phys. Lett. **430**, 355 (2006); M. Paulsson, T. Frederiksen, and M. Brandbyge, Nano Lett. **6**, 258 (2006); L. J. Yan, Phys. Chem. A **110**, 13249 (2006); A. Gagliardi, G. C. Solomon, A. Pecchia, T. Frauenheim, A. D. Carlo, N. S. Hush, and J. R. Reimers, Phys. Rev. B **75**, 174306 (2007); M. Kula and Y. J. Luo, Chem. Phys. **128**, 064705 (2008); M. Paulsson, C. Krag, T. Frederiksen, and M. Brandbyge, Nano Lett. **9**, 117 (2009).
[7] J. Hihath, C. R. Arroyo, G. Rubio-Bollinger, N. Tao, and N. Agraït, Nano Lett. **8**, 1673 (2008).
[8] The GAUSSIAN 09 Revision: A.02 code was used with the B3PW91 hybrid functional and Lanl2DZ basis. The functional PBE0(PBE1PBE) was used for comparison.
[9] A. Troisi, M. A. Ratner, and A. Nitzan, J. Chem. Phys. **118**, 6072 (2003).
[10] G. Kirczenow, P. G. Piva, and R. A. Wolkow, Phys. Rev. B **72**, 245306 (2005), P. G. Piva, R. A. Wolkow, and G. Kirczenow, Phys. Rev. Lett. **101**, 106801 (2008).
[11] H. Dalgleish and G. Kirczenow, Phys. Rev. B **72**, 155429 (2005); G. Kirczenow, *ibid.* **75**, 045428 (2007).
[12] D. M. Cardamone and G. Kirczenow, Phys. Rev. B **77**, 165403 (2008).
[13] J. H. Ammeter, H.-B. Bürgi, J. C. Thibeault, and R. Hoffman, J. Am. Chem. Soc. **100**, 3686 (1978).
[14] YAEHMOP numerical package by G. A. Landrum and W. V. Glassey, Source-Forge, Fremont, California, 2001.
[15] S. Datta, W. D. Tian, S. H. Hong, R. Reifenberger, J. I. Henderson, and C. P. Kubiak, Phys. Rev. Lett. **79**, 2530 (1997); E. G. Emberly and G. Kirczenow, *ibid.* **87**, 269701 (2001).
[16] J. Kushmerick, D. Holt, J. Yang, J. Naciri, M. Moore, and R. Shashidhar, Phys. Rev. Lett. **89**, 086802 (2002).
[17] J. Buker and G. Kirczenow, Phys. Rev. B **78**, 125107 (2008).
[18] J. Buker and G. Kirczenow, Phys. Rev. B **72**, 205338 (2005).
[19] S. M. Lindsay and M. A. Ratner, Adv. Mater. **19**, 23 (2007).
[20] Image made using MACMOLPLT; B. M. Bode and M. S. Gordon, J. Mol. Graphics Modell. **16**, 133 (1998).
[21] X. L. Li, J. He, J. Hihath, B. Q. Xu, S. M. Lindsay, and N. J. Tao, J. Am. Chem. Soc. **128**, 2135 (2006).